Management of metal chlorides in high temperature processes—Application to the nuclear wastes treatment

Florent Lemont *

French Atomic Energy Commission – CEA, Marcoule – DTCD/SCDV/LPIC, BP17171, 30207 Bagnols sur Cèze, France

ABSTRACT

Thermal processes are now the benchmark for the destruction of some waste whose toxicity requires special attention and management. Over many years the *Commissariat à l'Énergie Atomique* (French atomic energy commission) has developed technologies to process radioactive waste containing many metals together with chlorine, and thus with a major risk of producing volatile chlorides with potentially catastrophic effects on plant facilities. To mitigate these difficulties in an incineration process for radioactive waste contaminated by plutonium (IRIS), the CEA has investigated the processes by which potentially hazardous compounds are produced in order to eliminate them or prevent their formation. The studies have led to propose a phosphate-based stabilization technique thanks to an addition of phosphorus in the waste. Through a reaction occurring in gas phase, the metals are stabilized under a phosphate form when the formation of volatiles chlorides is avoided. While this technique has substantially improved process maintenance and security, it has revealed other difficulties related to potentially large phosphate deposits capable to cause unacceptable pressure drops detrimental to the gas flow conditions. This article describes the results of recent studies seeking to prevent the formation of volatile chlorides and phosphate deposits liable to obstruct the system flow lines.

1. Introduction – the IRIS process and the elimination of chlorides

To treat organic waste contaminated by α-emitting actinides from glove boxes in the nuclear industry, the CEA has developed an incineration process named after its pilot facility, IRIS (Installation for Research on Incineration of Solids). Fig. 1 is a general overview of the process.

IRIS is a three-step process implemented in rotating kilns [1]. The first step consists in oxidative pyrolysis at 550 °C, producing pitch that is then processed in a calcining step at 900 °C in oxygen-enriched atmosphere. The off-gases arising from the thermal treatments include a volatile hydrocarbon fraction that is oxidized at 1100 °C in an afterburner. A multistep process has two advantages. The elimination of chlorine at low temperature in the pyrolyzer limits corrosion problems and allows operation with low gas flow, which also limits particle entrainment. Adding oxygen during the pyrolysis step oxidizes the heavy hydrocarbons that produce tars capable of forming deposits in the ducts. Forming during the pyrolysis step, the pitch drops into the calciner being a rotary kiln heated at 900 °C. The pitch remains around 2 h in this furnace and is transformed into a ash having a very low carbon content

(<1%). On leaving the afterburner, the gases are carried to a very high-efficiency treatment system with filter stages to trap the solid particles transported and thus all the α-emitting actinides. Before discharge to atmosphere, the gas stream is submitted to caustic scrubbing to eliminate the volatile acids.

The material balance in the process is about as follow: a feeding rate of 4 kg/h produces around 1550 g/h of pitch, 111 g/h of ashes and 47 g/h of dust.

Although this technology limits corrosion, it does not completely prevent the production of metal chlorides. However, both thermochemical analysis and experimental findings show that the presence of oxygen in process systems favors the formation of silicates or aluminates rather than chlorides. Only volatile zinc chloride is formed in significant quantities, resulting in a very high chlorine concentration in the particulates. In general, the presence of element likely to react with chlorine to form volatile chloride will have a similar effect. This is the case for zinc, but also for lead, cadmium, etc. The particle matter appears to contain more than 95 wt% zinc chloride, which is very detrimental to the process facilities because this extremely hygroscopic product becomes deliquescent when exposed to ambient air. In this form it has a corrosive action that leads operators to maintain the facilities at high temperature even when they are not in use. One means of avoiding this difficulty is to convert the chlorides into more stable compounds. In earlier work [2] chloride ions were successfully replaced by phosphate ions, yielding much more stable and nonvolatile phosphate

* Tel.: +33 04 66 79 18 15.
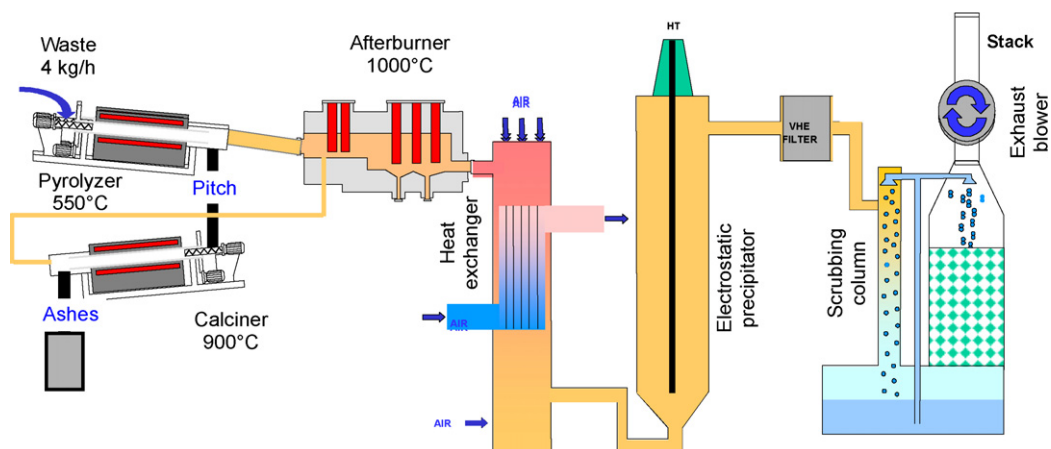*E-mail address:* Florent.lemont@cea.fr

Fig. 1. Schematic representation of the IRIS process.

compounds. This was done by introducing a compound such as tributyl phosphate (TBP) in the pyrolyzer or by using the phosphorus contained in a waste component.

Although this technique is effective, it modifies the physico-chemical nature of the compounds transported in the process, resulting in the appearance of localized deposits that may have negative effects on process control. Eliminating them or limiting their occurrence is a major issue today, and will require a better understanding of the mechanisms involved in their formation.

The present paper exposes in its different parts and through experimental and theoretical approaches, the main results obtained regarding the understanding of the behavior of several mineral embedded in hazardous waste and gives some proposals to upgrade the running of thermal processes. If the studies have been performed on the specific case of the IRIS process, the results may be very helpful for all other kind of thermal processes involving plasma torches or other heating means.

2. Behavior of mineral loads in a thermal process such as IRIS

2.1. Moderate-temperature pyrolysis step

2.1.1. Experimental and calculated results

The studies were carried out on an average composition representative of glove box waste from a Mixed OXide fuel (MOX) production facility. The waste composition is indicated in Table 1.

The difference between PVC-1 and PVC-2 lies in the much higher phosphorus content of the former. This material can be used for the phosphate treatment described above, although other liquid or solid compounds can of course also be used. Table 2 shows the results of a detailed elemental analysis of the waste composition.

The behavior of the elements within the process was initially assessed through thermodynamic equilibrium calculations based on minimizing the free enthalpy of the system, using FactSage® V.5.4.1 software to simulate the equilibria. With a database of about 4500 identified compounds, it determines the minimum chemical potential considering that the material balance must be conserved and the quantity of each species must be non-negative. The parameters taken into account are those indicated in Fig. 1, and the operating pressures are assumed equal to 1 atm.

Material input is based on the initial system composition for 4 kg of waste per hour, and cerium oxide CeO_2 was added to simulate plutonium behavior. Table 3 shows the molar composition of the simulation mixture. Fig. 2 indicates the nature of the compounds likely to form during pyrolysis, and allows their formation to be estimated as a function of the temperature.

This type of simulation shows that if the system is allowed to remain at equilibrium, a complex mixture of silicates, phosphates and chlorides would form. The equilibrium is not reached because of low kinetics but also because of interactions between compounds. Thus, it is interesting to compare these calculated results (Table 4) with analyses of the char from the first step of the process.

For most of the elements the simulations and analysis results are relatively consistent except for chlorine, for which the actual concentration was much higher than the equilibrium value. It is assumed that this difference is mainly due to the fact that chlorine is a heteroelement found in polymers (like sulfur) having relatively complex degradation mechanisms. Studies are now in progress to understand several phenomena that can lead to equipment malfunctions. The initial results confirm that some polymers such as neoprene or PVC subjected to a temperature increase may have complex degradation behavior. In the case of neoprene, for example, thermogravimetric analysis [3] showed such complexity, with polymer degradation beginning at temperatures between 500 and 600 °C depending on the heating rate. The delay, which is related to the presence of sulfur stabilizing the polyisoprene structure, shows that the pyrolysis temperatures and residence times of the IRIS process may be insufficient.

2.1.2. Interaction between gases and pitch – the case of ZnCl₂

The main issue of this work is to find one way to avoid the formation of zinc chloride in the thermal process and thus to understand the mechanism leading to its formation and release. Table 4 shows that a large amount of chlorine is driven toward the calcinatory when it was suppose to go directly to the afterburner. If one part of it may remain in unpyrolyzed plastic, one other can be adsorbed on the surface of the pitch produced in the pyrolysor.

Indeed, in addition to these degradation processes, it is important to consider the conditions in which certain gaseous species

Table 1
Representative average waste composition.

Component	wt%
PVC-1	19
PVC-2	12
Latex	17
Neoprene	17
EVA	25
Cotton	5
Kleenex®	5
Total	100

Table 2
Waste elemental composition.

Element	C	H	Cl	O	Al	Zn	Si	S	N	P	Ca	K	Ba	Na	Sb
wt%	60.61	8.41	16.36	9.55	0.66	0.54	0.48	0.43	0.40	0.23	0.19	0.14	0.04	0.04	0.03

Table 3
Initial system composition.

Element	Al	Ar	Ba	C	Ca	Ce	Cl	H
Quantity (mol)	0.978	224	0.012	202	0.190	0.033	18.460	336.400
Element	K	Na	O	P	S	Si	Zn	
Quantity (mol)	0.143	0.069	113.160	0.297	0.540	0.680	0.330	

Table 4
Equilibrium calculations (550 °C) versus process analysis results for char from the IRIS process (wt%).

	C	Al	Si	Zn	S	P	K	Na	Cl	Ca	Ba	Ce
Calculated	90.96	1.39	1.01	0.9	0.44	0.48	0.29	0.08	0.48	0.40	0.09	0.24
Experimental	84.20	1.62	1.12	1.23	0.67	0.10	0.72	0.17	4.51	0.59	0.14	0.14

are generated in the pyrolysis step. The surface of the pitch being formed may be activated to some extent. The volatilization of some species such as chlorides [4] will therefore be influenced by their adsorption on the solid and their accumulation in its pores. In this case, mass transfer to the surrounding environment of a gaseous species partially adsorbed in a carbonaceous solid must be considered. This approach must allow for such mechanisms, described in a particle of radius r by the following expression:

$$\rho_p \frac{\partial q}{\partial t} + \varepsilon_p \frac{\partial C}{\partial t} = D_e \left(\frac{\partial^2 C}{\partial r^2} + \frac{2}{r} \frac{\partial C}{\partial r} \right) \tag{1}$$

where ρ_p is the bulk density of the solid, q the concentration of gaseous species adsorbed, ε_p the particle porosity, D_e the diffusivity, C the concentration of the gaseous species in the pores, and r the particle center radius.

If the adsorbing solid/mineral vapor system is assumed to reach equilibrium, this expression can be simplified by introducing a pseudo-diffusion coefficient D^*:

$$\frac{\partial C}{\partial t} = D^* \left(\frac{\partial^2 C}{\partial r^2} + \frac{2}{r} \frac{\partial C}{\partial r} \right) \quad D^* = \frac{D_e}{\varepsilon_p + \rho_p(\partial q/\partial C)} \tag{2}$$

The pseudo-diffusion coefficient D^* can be assumed constant (isothermal equilibrium) and $q = KC$, where K is the adsorption constant.

Allowing for radiative transfers at each particle [4], for which the expression is similar to Eq. (2), the change in the quantity of inorganic vapor in the solid is given by the following expression:

$$\frac{\bar{q}(t)}{q_0} = \frac{6}{\pi^2} \sum_{n=1}^{\infty} \frac{1}{n^2} e^{(-n^2 \pi^2 D*t/R^2)} \tag{3}$$

$\bar{q}(t)$ is the mean metal concentration in each particle, and is defined as follows:

$$\bar{q} = \frac{3}{R^3} \int_0^R qr^2 dr \tag{4}$$

In this approach, D^* must be determined from the diffusivity coefficient D_e calculated from the diffusion coefficient D as follows:

$$D_e = \frac{\varepsilon_p}{\tau_p} D \tag{5}$$

ε_p is the material porosity and τ_p its tortuosity. Specific studies of the structure of char particles [5] gives values of 0.55 and 1.41, respectively.

D is calculated by comparing the mean free path l of a gas molecule (in this case $ZnCl_2$) and the mean pore radius δ; l is calculated from following expression:

$$l = \frac{RT}{\pi \sqrt{2} P N \phi^2} \tag{6}$$

where P is the total pressure (1 atm) and ϕ the mean diameter of the molecule. As $ZnCl_2$ is linear and ionic, ϕ is about 0.87 nm. Hence l can be estimated at about 33 nm.
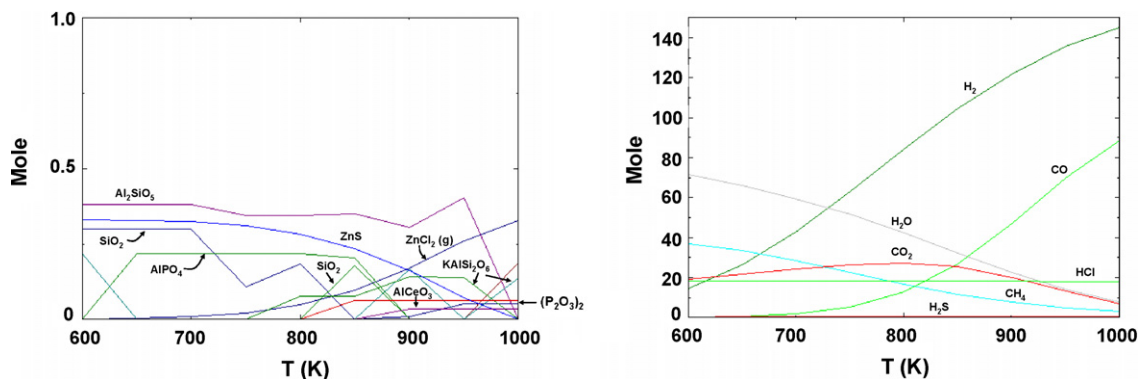

Fig. 2. Equilibrium system composition versus temperature (Left: solids; Right: gases).
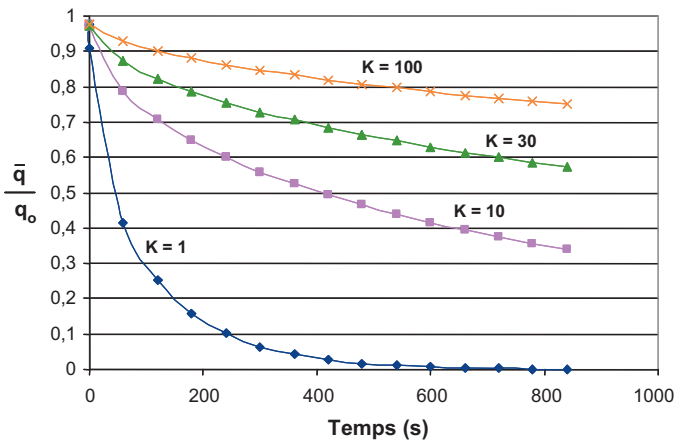
Fig. 3. $\bar{q}/q_0$ ratio as a function of time and of the adsorption constant K.

BET porosimetry measurements give a mean pore radius of 15 nm (corroborated by Eghlimi et al. [5]). Thus l and δ are of comparable magnitude, allowing D to be calculated from the following expression:

$$\frac{1}{D} = \frac{1}{D_K} + \frac{1}{D_m} \qquad (7)$$

D_K (the Knudsen diffusivity) is calculated using the following equation:

$$D_K = \frac{1}{3}\delta\sqrt{\frac{8RT}{\pi M}} \qquad (8)$$

As M is the molar mass of zinc chloride ($136.29\,\text{g mol}^{-1}$), $D_K = 1.79 \times 10^{-6}\,\text{m}^2\,\text{s}^{-1}$.

The molecular diffusion coefficient of zinc chloride at 550 °C is not known but may be approximated from the data for mercury chloride [4] using the following expression:

$$D_{ZnCl_2}^{550\,°C} = \left(D_{HgCl_2}^{600\,°C} - \frac{D_{HgCl_2}^{850\,°C} - D_{HgCl_2}^{600\,°C}}{5}\right)\sqrt{\frac{M_{HgCl_2}}{M_{ZnCl_2}}} \qquad (9)$$

This calculation gives $D_{ZnCl_2}^{550\,°C} = 7.7 \times 10^{-5}\,\text{m}^2\,\text{s}^{-1}$; D can thus be calculated from expression (7), giving $D = 1.75 \times 10^{-6}\,\text{m}^2\,\text{s}^{-1}$ and $D_e = 6.8 \times 10^{-7}\,\text{m}^2\,\text{s}^{-1}$.

The adsorption constant K in this expression is unknown. However, the evolution of the $\bar{q}/q_0$ ratio as a function of this constant can be observed. The results of this approach are indicated in Fig. 3.

Table 5
Elements supplied to the calciner.

Compound	Quantity (mole)
C	143.74
Al_2SiO_5	0.359
$ZnCl_2$	0.262
Al_2O_3	0.092
SiO_2	0.167
$Al_2Si_2O_6$	0.075
NaCl	0.069
$Ca_5P_3O_{13}H$	0.038
K_2CeCl_5	0.033
$BaCl_2$	0.012
O_2	89.286
Ar	178.57

It appears that the volatilization of zinc chloride, which can be expressed by $1 - \bar{q}/q_0$, is strongly dependent on the value of K. For example, the values for silica, clay and alumina are respectively about 6, 24 and 37; the value for the IRIS char (activated charcoal) is thus presumably situated at a higher level. However, Fig. 3 shows that for a value of 30 and a processing time of 5 min (300 s, the average pyrolyzer residence time), $ZnCl_2$ volatilization does not exceed 30% of the initial content. Even if the processing time is significantly extended, it is obvious that 50% will be difficult to achieve. This type of behavior has already been observed in other applications [6], and incites us to reconsider the routing of volatile metallic species in the process via the calciner before reaching the afterburner.

Both the experimental and computational results concerning the pitch composition indicated in Table 4 show that zinc tends to remain in the solid. Indeed, for a feeding rate of 4 kg/h of waste and thus 22 g/h of zinc, the flow rate of zinc going with the pitch is 19 g/h when its flow rate in the gases is 3 g/h. Fig. 2, showing a state of equilibrium, indicates that it would be in the form of ZnS. The data in Table 4 indicate rather a chloride form. Comparing this result with studies of the degradation kinetics of neoprene or latex containing all the sulfur [3] shows that zinc remains largely adsorbed in the pores of the char as $ZnCl_2$. Additional analysis consisting to leach the pitch 48 h with pure water shows that 97 wt% of zinc is soluble. Contrary to zinc chloride $ZnCl_2$, the zinc sulfide ZnS is not soluble in water attesting that the zinc is well under the chloride form.

2.2. High-temperature calcining step

The residence time for the calcining step is about 2 h, allowing the system to approach thermodynamic equilibrium. An operation
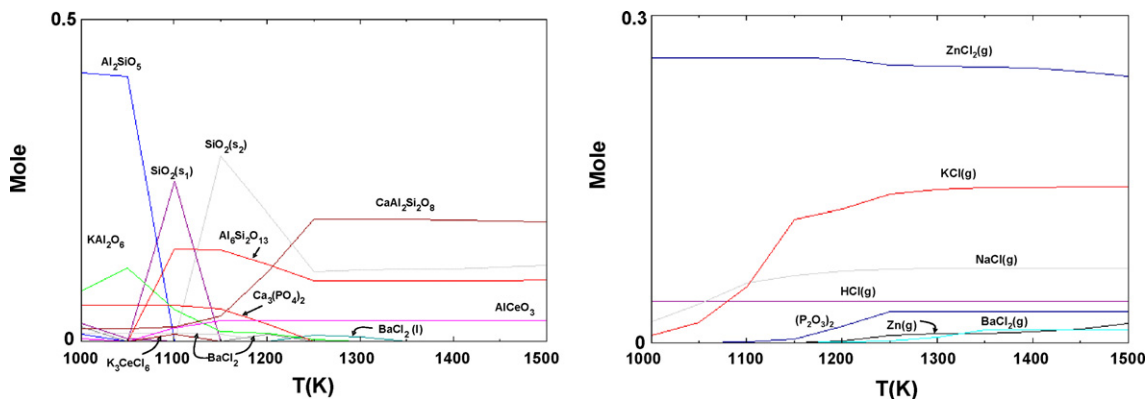

Fig. 4. Equilibrium system composition versus temperature (Left: solids; Right: gases).

Table 6
Equilibrium calculations versus process analysis results for ashes from the IRIS process (wt%).

	C	Al	Si	Zn	S	P	K	Na	Cl	Ca	Ba	Ce
Calculated	0	21.93	16.46	0	0	2.32	0.50	0	0.65	6.56	1.39	3.98
Experimental	0.35	17.00	12.40	0.58	0.15	1.08	2.86	0.87	0.41	7.59	0.98	2.67

similar the one carried out for pyrolysis was performed using the results obtained during the first simulation, with two corrections:

- Zinc introduced in the form of $ZnCl_2$ instead of ZnS.
- Aluminum in the form of $AlPO_4$ was introduced as Al_2O_3 to approximate the experimental concentrations in Table 4.

Table 5 indicates the quantities of solids entering the calciner according to the results obtained previously. (Gases required for the treatment such as O_2 and Ar have been taken into consideration for the calculation and then appear in the table.)

The system evolution according to the temperature is shown in Fig. 4.

The solid species formed show a relatively stable system completely devoid of carbon, with a possible emergence of liquids that could disrupt system operation. These liquids can be pure (e.g. $BaCl_2$) or specific compounds not listed above. Concerning the gases, $ZnCl_2$ is completely vaporized, and other gaseous species such as KCl or NaCl appear. The comparison with experimental results shows very strong $ZnCl_2$ volatilization from the calciner, which can condense in the ducts resulting in serious maintenance problems. Table 6 compares the results of equilibrium calculations with the experimental results.

Table 6 shows that the ash quality obtained generally corresponds to the results of a simple equilibrium calculation. The most significant differences concern volatilized zinc and sodium, and can be explained through an approach similar to the previous one, as well as through zinc speciation different from $ZnCl_2$ and not present in the database. For example, X-ray diffraction analysis of the ashes not only confirmed the presence of aluminosilicates, but also revealed traces of ZnS and phosphates. The quantity of mineral collected during an incineration campaign was about 110 g/h, compared with the computational speciation results of 116 g/h, which is very satisfactory for an industrial application.

Today the theoretical and experimental results regarding the evolution of the mineral load during the first two stages of the incineration process are relatively satisfactory, and allow us to

understand the mechanisms controlling the gas composition and the phenomena observed in and downstream from the afterburner.

3. Optimizing the phosphate treatment

3.1. Conventional phosphatation

As indicated in the process description, the introduction of phosphorus should allow conversion of the volatile chlorides into phosphates. It can be added either as organic liquid such as tributyl phosphate (largely used in nuclear industry as actinides extractant) directly into the pyrolysor [2] or under other liquid form (Ammonium Hydrogeno Phosphate, Tri Aryl Phosphate, . . .). Whatever the chosen way, previous studies [2] have shown that the addition of phosphorus to the incinerable waste stream in stoichiometric proportions with zinc ($X_P/X_{Zn} \geq 0.7$) results in virtually complete conversion of zinc chloride to zinc phosphate. This conversion effectively occurs, since the particles collected on the filters consist mainly of zinc phosphate but it is only partial, because zinc chloride condenses between the pyrolyzer and the calciner, as this species is captured by the char. Analysis have been performed on sampling of deposits collected at different points of the process. They have permitted, together with the previous results, to propose a mechanism of phosphatation and thus to propose a flow diagram for the species involved in the phosphatation reaction (Fig. 5).

Other volatile species may be involved in this process, of course. The analyses showed that potassium and sodium are present in the particles, which is consistent with the gas compositions indicated in Fig. 5. In agreement with the theoretical analysis and the experimental results, phosphatation of the volatile reactive species occurs in the afterburner and produces a compound assumed to be zinc orthophosphate $Zn_3(PO_4)_2$. Speciation studies have shown that while this species is indeed found in the particles, other polyphosphates such as $Zn_2P_2O_7$ or $Zn_5(P_3O_{10})_2$ are also present. The X-ray diffraction diagram of the particulates in Fig. 6 reveals peaks associated with orthophosphate together with other peaks associated with various phosphates. This characterization was carried out on a
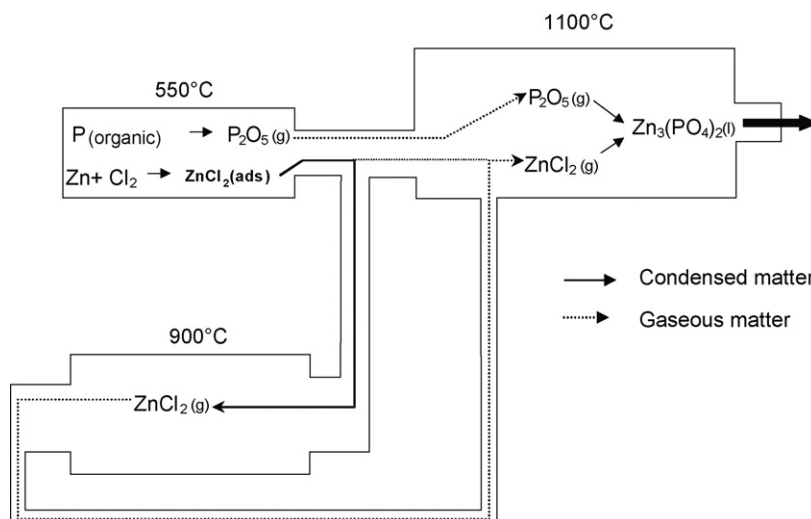

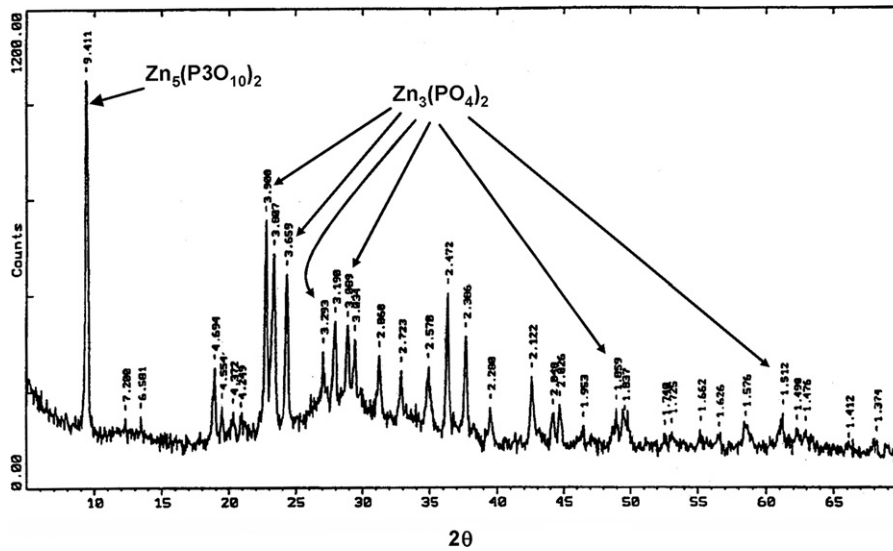
Fig. 5. Phosphorus and zinc flows in the IRIS process.

Fig. 6. X-ray diffraction diagram of electrostatic precipitator dust sample.

Brüker AXS D8 Advance diffractometer (λ_{Cu} = 1.5406 Å). The diffractogram were compared to the ICDD base data.
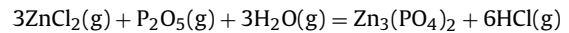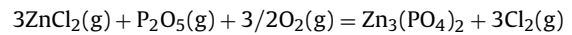
These mixtures – whose composition depends directly on the reactive conditions in the afterburner (temperature, pressure, Zn/P ratio, etc.) and on the cooling conditions – can lead to systems having characteristics incompatible with optimum process operation. For example studies on systems limited to the pseudo-binary ZnO–P_2O_5 [7] were used to define a phase diagram with several identified compounds (Fig. 7) and high anhydride concentrations resulting in low melting points.

The phase diagram shows that whatever the compound(s) formed in the afterburner, the system will have fluxing properties and will thus easily form deposits. Since the phosphating reaction occurs in the gas phase, it produces a mist of phosphate microdroplets in suspension in the off-gas stream. They can impact the furnace well and remain liquid, or impact and solidify on the afterburner outlet duct. Observations in the facility showed major deposits [8] in the furnace outlet that were too crystallized to be analyzed by X-ray diffraction. However, elemental analysis confirmed that they were zinc phosphates.

3.2. Addition of phosphorus in the calciner

The work just described on the incineration behavior of the waste mineral load was the basis for proposing and implementing technological developments destined to improve the overall process. The prior studies showed that zinc chloride, resulting from the combination of chlorine from PVC and zinc from neoprene, is adsorbed and enters the calciner where it is volatilized and transferred to the afterburner (Fig. 5). The phosphating reaction occurs in the afterburner to produce zinc phosphate, whose composition can vary depending on the quantity of phosphorus in the system (Fig. 7). While the phosphate treatment substantially diminishes or even eliminates zinc chloride, it produces compounds that may be liquid and thus form deposits that can disrupt fluid flow. Studies were undertaken to assess the feasibility of performing phosphatation directly in the calciner, in which the residence times and temperatures can be sufficient to ensure chemical conversion. The thermodynamic approach cannot be limited to the formation of zinc orthophosphate $Zn_3(PO_4)_2$, as no data are available concerning pyrophosphates $Zn_2P_2O_7$ or $Zn(PO_3)_2$ or polyphosphates. The study can be limited to investigating the evolution of the following systems:

$$3ZnCl_2(g) + P_2O_5(g) + 3/2O_2(g) = Zn_3(PO_4)_2 + 3Cl_2(g)$$

$$3ZnCl_2(g) + P_2O_5(g) + 3H_2O(g) = Zn_3(PO_4)_2 + 6HCl(g)$$

In both cases, an advanced degree of reaction progress is reached and the equilibria can be considered complete. When the equilibrium constants are plotted versus the temperature (Fig. 8) in order to illustrate the reaction progress, a lower temperature can be seen to favor the thermodynamics of the reactions.

As in the case of pyrolysis, the chemical systems involved in calcination are relatively complex; phosphate cross reactions and
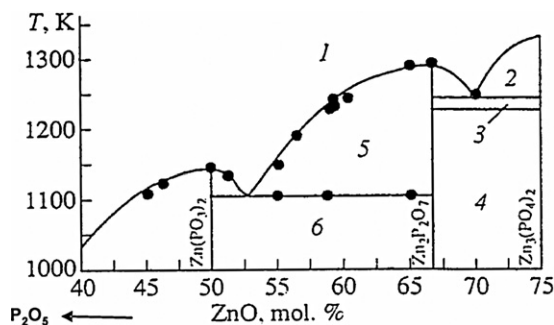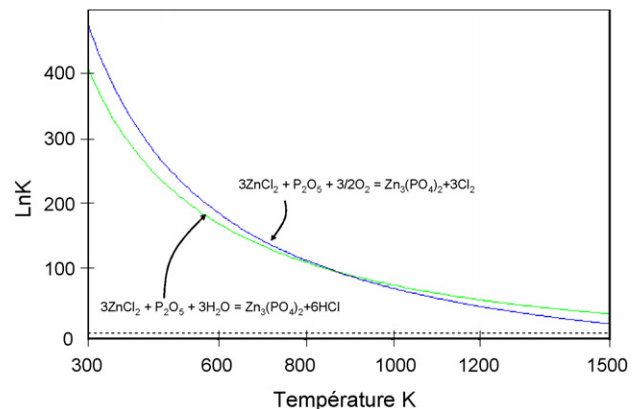

Fig. 7. ZnO–P_2O_5 phase diagram [7].

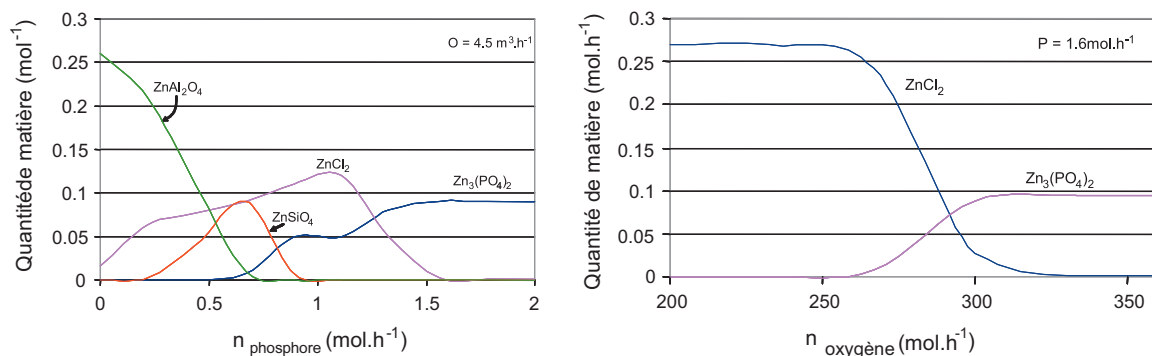**Fig. 8.** Phosphatation reaction progress versus temperature.

Fig. 9. Zinc speciation at 800 °C versus phosphorus and oxygen concentrations in the calciner.

interactions between elements should be taken into account. Work recently initiated in this area will take into account the multiple interactions and physicochemical behavior of the mineral species produced.

In the event that phosphatation is carried out in the calciner, the pitch composition supplied to the furnace would be modified to eliminate phosphorus in the feed stream. The recalculated composition pitch would then be in Table 7.

The degree of phosphatation will of course depend on the phosphorus content, but also on the quantity of oxygen introduced, which will determine the oxidizing properties of the calciner environment. In the case of an oxygen deficit, the reducing conditions characterized by a high CO content will limit phosphatation by constraining phosphorus to P_2O_3 and/or P_4O_6. Excess oxygen relative to carbon will create a sufficiently oxidizing environment to ensure phosphatation of zinc as $Zn_3(PO_4)_2$ or in a form richer in phosphorus such as $Zn_2P_2O_7$. Based on orthophosphate, the only form present in the databases, the evolution of zinc-based compounds was calculated and is shown in Fig. 9 (to ensure that $Zn_3(PO_4)_2$ is included, the calculations were performed with the Thermodata database- Coach Bank 00 V06-00). In this case an optimum operating point appears, corresponding to a feed rate of 1.6 mol per hour of phosphorus (calculated for a waste feed rate of 4 kg/h) and about 300 mol of oxygen, i.e. an oxygen flow rate of about 3.4 $Nm^3 h^{-1}$.

The conversion of zinc chloride to phosphate is optimized for the process if the reaction medium contains sufficient hydrogen to produce hydrogen chloride instead of chlorine Cl_2. Adding phosphorus in the form of an organic compound such as TBP ($C_{12}H_{27}PO_4$) ensures this conversion. The studies carried out showed that the quantity of hydrogen supplied by this compound is sufficient to diminish the chlorine concentration to very low levels and ensure optimum conversion of chlorine to HCl, which is then neutralized in the scrubbing columns.

While the studies undertaken with respect to phosphatation in the calciner involve chemistry, they must also be accompanied by

technological changes in the entire process because a large quantity of fine particles will be released from the furnace. To prevent them from reaching the afterburner where they would be melted, it is therefore necessary to implement a suitable retention system such as a cyclone separator or electrostatic precipitator. The additional cost imposed by this implementation will be offset by the possible reduction of the size of the filtering equipments (a large part of the dust will be recovered together with the ashes) and also thanks to the protection of the equipment guarantee by the elimination of the chlorinated compounds.

The initial tests have shown effective phosphate treatment in the furnace tube with significant recovery of phosphate particles. A few easily removable deposits are observed in the calciner which are related to the appearance of mixtures melted in the furnace. A theoretical analysis of the ashes obtained for incineration optimized as described above indicates the production of a complex mixture with the approximate composition provided in Table 8.

Later experiments, carried out with the same wastes, have been followed by analysis performed on ashes, dusts and deposits. The deposits, exclusively present in the very first zone of the rotary kiln was an almost melted mixture, easy to recover.

Table 9 provides the theoretical composition of the ashes (from Table 8) and the experimental compositions of ashes, deposits and dusts.

The oxygen composition has not been analyzed explaining why it does not appear in the table. The table shows a rather good agreement between the calculation and the analysis for the ashes except for the chlorine that can react with other element than Zn before released in the gas stream.

Even if the speciation of each element has not been performed, it was interesting to compare the ratios between ($n_{Al} + n_{Ca} + 1.5n_{Zn} + n_{Na}$) and n_P to be consistent with Table 8. The results show a ratio of 0.7 for the deposits, 0.9 for ashes and 2.7 for the dusts that contain no more than 1 wt% of chlorine (0.7 mol%) testifying a good efficiency of the reaction. It is interesting to note that the sodium and zinc contents in the deposits is much more higher than in the ashes. This may explained why the deposits are almost a melted mixture.

Table 7
Composition of pitch without phosphate treatment prior to calcination.

Element	Quantity (mol h^{-1})	Estimated compound	Quantity (mol h^{-1})
C	142.2	Al_2SiO_5	0.263
Al	0.976	$CaAl_2Si_3O_{10}(OH)_2$	0.117
Si	0.681	$ZnCl_2$	0.273
Ca	0.190	K_3AlCl_9	0.047
Zn	0.272	$Ca_2Al_2SiO_7$	0.037
K	0.142	Na_2AlCl_6	0.034
Cl	0.657	$Ce(SO_4)_2(5H_2O)$	0.033
Na	0.069	$Al_2O_3SiO_2$	0.030
Ce	0.033	$BaCl_2$	0.012
Ba	0.012		

Table 8
Ash composition in the furnace.

Compound	Concentration (mol h^{-1})
$AlPO_4$	0.98
SiO_2	0.66
$Ca_2P_2O_7$	0.095
$Zn_3P_2O_8$	0.09
CeO_2	0.03
$Na_4P_2O_7$	0.017
$BaSi_2O_5$	0.012

Table 9
Theoretical and experimental composition for ashes, deposits and dusts.

Element	Ashes theoretical composition (wt%)	Ashes experimental composition (wt%)	Dusts experimental composition (wt%)	Deposits experimental composition (wt%)
Al	11.5	7.5	6.8	3
P	18.6	17.5	9.8	20
Si	8.3	8.8	12.3	8.8
Ca	3.3	4.1	9.3	3.3
Zn	7.6	11.6	11.4	22
Ce	1.8	2.1	1.8	2
Na	0.7	0.9	3.2	2.2
Ba	0.7	0.3	0.4	0.4
Cl	0	0.8	1	1.2
O	47.5	–	–	–
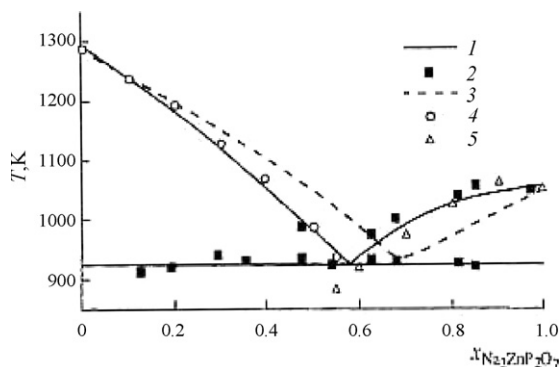
Fig. 10. Liquidus curves for $Zn_2P_2O_7$–$Na_2ZnP_2O_7$ system. 1: Diagram proposed by Felnner et al. [9,10], 2: experimental data points obtained DSC [9], 3-4-5: diagram obtained by different models [9].

Indeed, mixture of phosphates and oxides (including silica) can lead to the formation of compounds with low melting points that tend to sinter easily. Prior work on the production of phosphate-based composites [9] demonstrated the formation of defined compounds in which alkali metals tended to lower the melting points appreciably. For example, the presence of sodium in our application could result in the formation of a mixed $Na_2ZnP_2O_7$ compound with a melting point of about 780 °C, as shown on the phase diagram in Fig. 10.

The composition data show that the system obtained in the calciner is probably located in areas richer in sodium, accounting for the possibility of obtaining low melting points leading to the formation of retentions.

4. Conclusion

The management of metals is a major issue in a thermal process for waste treatment, and they must be stabilized as far as possible. This issue becomes crucial when the metals form volatile compounds by combining with elements such as chlorine.

For the treatment of radioactive organic waste, experience has shown that the combined presence of zinc and chlorine generates zinc chloride, whose volatility results in the formation of very corrosive deposits in the off-gas treatment system. An excellent way to overcome this problem is to convert the gaseous chlorides into phosphates, much more stable and noncorrosive compounds. In this context, a protocol was developed to carry out this conversion in the IRIS process in two steps, first at moderate temperature and then at high temperature.

The mechanism initially contemplated was volatilization of the phosphorus and zinc in the first step, with recombination in the afterburner heated to 1100 °C. Experimentation showed that the volatile element transfer mechanisms are not so simple, and must allow for the adsorption properties of the char in the heart of the process. These properties radically modify the pathways of the compounds, as well as their formation and deposit zones. It is therefore of fundamental importance to study and assess these properties to optimize the processes and help stabilize the corrosive or hazardous compounds.

The application of this study to zinc present in radioactive organic waste incinerated by the IRIS process demonstrated that zinc chloride does not volatilize in the initial pyrolysis step but rather during subsequent calcining where phosphorus is not present to ensure phosphatation. A modification of the procedure for phosphatation of the volatile chlorides was therefore proposed to shift the reaction to the optimum location. When carried out in the zinc chloride desorption zone – i.e. in the calciner – it is highly effective and protects the entire treatment facility.

References

[1] A. Jouan, J.P. Moncouyoux, R. Boen, R. Cartier, J.J. Vincent, T. Longuet, Incineration processes for radioactive waste with high alpha contamination: new developments, in: IT3 Conference, May 8–12th, Bellevue, Washington, USA, 1995, p. 209.
[2] H. Rouault, R. Cartier, R. Boen, T. Longuet, Phosphorus: in situ treatment for ZnCl₂, formed by incineration of organic waste, in: IT3 Conference, May 11–15th, 1998, p. 225.
[3] J.A. Caballero, J.A. Conesa, I. Martin-Gullon, R. Font, Kinetic study of the pyrolysis of neoprene, Journal of Analytical and Applied Pyrolysis 74 (2005) 231–237.
[4] S. Abanades, G. Flamant, D. Gauthier, Modelling of heavy metal vaporisation from a mineral matrix, Journal Hazardous Materials B88 (2001) 75–94.
[5] A. Eghlimi, L. Lu, V. Sahajwalla, D. Harris, Computational modelling of char combustion based on the structure of char particles, in: Second International Conference on CFD in the Minerals and Process Industries, December 6–8, CSIRO, Melbourne, Australia, 1999.
[6] D. Marani, C.M. Braguglia, G. Mininni, F. Maccioni, Behavior of Cd, Cr, Mn, Ni, Pb and Zn in sewage sludge incineration by fluidised bed furnace, Waste Management 23 (2003) 117–124.
[7] S.I. Shornikov, A.L. Shilov, M.M. Shults, A mass-spectrometric study of the thermodynamic properties of ZnO–P₂O₅ system melts, Russian Journal of Physical Chemistry 70 (3) (1996) 447–453.
[8] J.Y. Poinso, C. Thiebaut, F. Lemort, J.P. Charvillat, The alpha waste incinerator at the CEA Valduc. Assessment and improvement of the active waste incineration, in: IT3 Conference, May 12–16th, Orlando, USA, 2003.
[9] V.M. Ushakov, N.V. Borisova, M.M. Shultz, A study of thermodynamic characteristics of the Zn₂P₂O₇–M₄P₂O₇ (M = Li and Na) systems by differential scanning calorimetry, Glass Physics and Chemistry 27 (3) (2001) 259–266.
[10] P. Felnner, J. Majling, Calculation of liquidus curves in phase diagrams Na₄P₂O₇–Mg₂P₂O₇ and Na₄P₂O₇–Zn₂P₂O₇, Chem. Zwesti 27 (6) (1973) 728–731.